Enhancement of hydrogen response by forming an Au submonolayer on nanogap Pd nanoparticles

Nobutomo Nakamura,[1, a)] Kazushi Yoshikawa,[1] and Akio Ishii[2]

[1)] *Graduate School of Engineering, Osaka University, 2-1 Yamadaoka, Suita, Osaka 565-0871, Japan*

[2)] *Graduate School of Engineering Science, Osaka University, 1-3 Machikaneyama, Toyonaka, Osaka 560-8531, Japan*

When Pd nanoparticles dispersed on a glass substrate with nanometer order gaps are exposed to H_2 gas, H atoms are adsorbed on the nanoparticle surface, and the electrical resistance between the nanoparticles increases because of the tunneling current suppression. In contrast, when Au nanoparticles are exposed to H_2 gas, the resistance remains unchanged because H atoms are not adsorbed on the Au surface. Considering these behaviors, the change ratio of the electrical resistance is expected to be smaller when the surface of Pd nanoparticles is partially covered with Au. However, the experimental results show the opposite resistance change. Density functional theory simulation indicates that H atoms are adsorbed and absorbed on the pure Pd surface, but H atoms are adsorbed and tend to remain on the partially covered Pd surface. These results indicate that the decrease in the resistance due to the gap narrowing by hydrogen absorption occurs in Pd nanoparticles, but it does not occur in Au/Pd nanoparticles, resulting in a larger resistivity increase compared with the Pd nanoparticles. This result implies that in certain cases, the low reactivity of Au to H_2 contributes to the enhancement of the electrical resistance response.

[a)]Electronic mail: nakamura@mech.eng.osaka-u.ac.jp

When Pd is exposed to an atmosphere including H_2 gas, it adsorbs and absorbs the H atoms. Adsorption and absorption change the physical properties of Pd, and it has been applied to hydrogen-gas sensors.[1–3] One of the representative sensing mechanisms is the measurement of the electrical resistance change of Pd nanostructures; (i) the resistance of Pd increases because of H_2 absorption, (ii) the resistance decreases with contact of Pd nanostructures because of the volume increment by H_2 absorption, and (iii) tunneling current is suppressed by H_2 adsorption on the surface of noncontacting Pd nanostructures.[4–10] Because Pd-based alloys sometimes show properties superior to those of Pd, these alloys are also applied for such H_2-gas sensors.[11–13] Under these circumstances, in this study, we observed that resistance change in the tunneling-current based sensor is enhanced by using Pd nanoparticles partially coated with Au.

Several studies have demonstrated the unique properties of Au nanoparticles and alloys. When Au becomes nanoparticles with a diameter of a few nanometers or is attached as nanoparticles on the surface of oxides, it exhibits catalytic reactions with H_2.[14,15] For the response to H_2 gas, hysteresis disappears in plasmonic optical sensors using Pd-Au alloy nanoparticles[16], and the H_2 absorption rate increases when one atomic layer of Au is formed on the Pd (110) surface.[17] However, in general, Au shows low reactivity with H_2; no dissociative H_2 adsorption occurs over the smooth surfaces of Au at temperatures below 473 K.[14]

In this study, we performed H_2-gas sensing using nanogap nanoparticles and evaluated the effect of Au coating on Pd nanoparticles. This sensor is based on the tunneling-current change by H_2 adsorption. The main result of this study is that while Au on Pd nanoparticles exhibits an inherently low reactivity (H_2 adsorption and absorption are less favorable), it improves the performance of the tunneling-current based sensor. A feature that appears to be a disadvantage of Au works as an advantage in this sensor. We performed experiments on the H_2-gas detection. The experimental results were energetically analyzed using the density functional theory (DFT) simulations, and the effectiveness of Au coating on Pd nanoparticles was discussed.

The tunneling-current based sensor comprises Pd nanoparticles dispersed on a glass substrate. The nanoparticles are isolated on the substrate, and the gap size, the distance between the nanoparticles, is sufficiently small for the tunneling current to occur. Such nanoparticles are called nanogap nanoparticles. Nanogap nanoparticles can be synthesized

by sputtering. When metal is sputtered on a substrate, isolated nanoparticles are formed, and a continuous film is formed after they grow. Nanogap nanoparticles are obtained by interrupting the sputtering process immediately before the nanoparticles contact. However, detecting the moment at which nanoparticles are in contact is quite difficult. We addressed this issue by developing the resistive spectroscopy[18,19] and synthesized nanogap nanoparticles with different gap sizes.

Using resistive spectroscopy, nanogap Pd, Au, and Pd with Au coating (Au/Pd) nanoparticles were synthesized at room temperature on a glass substrate of 0.1-mm thickness with changing the gap size. In the sputtering, background pressure was less than 5.0×10^{-4} Pa, and Ar pressure was 0.8 Pa. The sputtering rates of Pd and Au were 0.016 and 0.02 nm/s, respectively. Pd and Au nanoparticles were synthesized by sputtering Pd and Au, respectively. Nanogap Au/Pd nanoparticles were synthesized by sputtering Au after synthesizing nanogap Pd nanoparticles, in which the thickness of Au was about 0.2 nm. The height of the nanoparticles ranges from 2.1 to 9.8 nm, which was calculated from the deposition rate and time. In face-centered-cubic (FCC) metal nanoparticles, (111) plane tends to appear on the nanoparticle surface because of its lower surface energy than other planes.[20] Assuming that the (111) plane of Au appears on the surface of the Au/Pd nanoparticles, the thickness of the sputtered Au becomes less than the interatomic distance, approximately 0.235 nm, and the surface of Pd nanoparticles is partially covered with Au.

In H_2-gas detection experiments, the electrical resistance on the substrate surface was measured using contact probes in the gas-flow cell. The measurement setup is described elsewhere[10,21]. N_2 gas flows into the cell as a carrier gas at a rate of 117 mL/min. Then, 1000-ppm H_2 gas in N_2 gas is added into the carrier gas at a rate of 13 mL/min, and H_2 gas of 100 ppm is detected by the nanoparticles. The flow path of the experimental system is evacuated before the hydrogen detection experiment to prevent the inclusion of impurity gases. The experiment was conducted at room temperature. Figure 1 shows the representative resistance change ΔR measured during the H_2-gas flow for 231 s. In Pd nanoparticles, when the initial resistance R_0, the resistance just before the H_2-gas flow starts, is relatively high ($\sim$MΩ), the resistance increases. This is because the H_2 adsorption on Pd nanoparticle surface suppresses the tunneling current between isolated Pd nanoparticles. However, the resistance decreases when the initial resistance is lower ($\sim$kΩ). This is because Pd nanoparticles are expanded by volume increment by H_2 absorption, which makes gaps be-

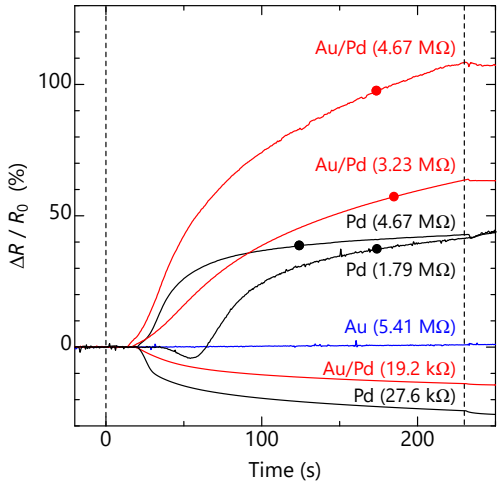

FIG. 1. Resistance change during H_2-gas flow for 231 s at 100 ppm. Dashed lines represent the time when the flow is initiated and interrupted. There is a time lag after initiating the flow. The numbers in parentheses represent the initial resistance R_0, and the dots denote the response time.

tween nanoparticles narrower and close, decreasing the resistance. Similar resistance changes were observed in Au/Pd nanoparticles. In contrast, the resistance of Au nanoparticles was unchanged by the H_2-gas flow.

Considering that H_2 is absorbed after it is adsorbed on the nanoparticle surface, the resistance was expected to initially increase during the H_2-gas flow; however, this was not observed on Pd and Au/Pd nanoparticles. We have previously performed hydrogen gas detection experiments on nanogap Pd nanoparticles with different gap sizes and observed that the behavior of the electrical resistance change varies with gap size[10]. For nanoparticles with sufficiently large gap size (higher R_0), the electrical resistance increases as seen on Pd (4.67 MΩ). This result indicates that hydrogen adsorbs on the nanoparticle surface, causing the electrical resistance to increase. On the other hand, when the nanogap becomes smaller, the electrical resistance first increased slightly, then decreased temporarily, and then increased again as seen on Pd (1.79 MΩ). Since the decrease is thought to be caused by the nanogap closing, this result suggests that hydrogen absorption occurs immediately after hydrogen flow. The increase in electrical resistance after the decrease suggests that hydrogen adsorption on the nanoparticle surface continues even after the nanogaps close.

Thus, hydrogen absorption does not necessarily occur after the surface is fully covered with hydrogen. The reason for the lack of a decrease in Pd (4.67 MΩ) is that the initial gap size was large, and the gap size was not reduced enough by hydrogen absorption to close the nanogap, so the rate of decrease in the electrical resistance was small. As the nanogap becomes even smaller, the decrease in electrical resistance due to gap closure becomes more pronounced, and no increase in electrical resistance is observed as seen on Pd (27.6 kΩ). Thus, it is expected that hydrogen adsorption and absorption occur simultaneously in the nanogap Pd nanoparticles, and depending on the size of the nanogap, the electrical resistance does not necessarily increase first.

Figure 2 shows the relationship between the initial resistance and the change ratio of the resistance after the H_2-gas flow for 231 s. As shown in the figure, the resistance change of Pd and Au/Pd nanoparticles depends on the initial resistance. The resistance change varies from increase to decrease as R_0 decreases ($1/R_0$ increases). In contrast, the resistance of Au nanoparticles remains almost unchanged by the H_2-gas flow, confirming that Au is less reactive with H_2 gas. Considering the difference between Pd and Au/Pd, no significant difference in the resistance change was observed for the gap-closing type response ($1/R_0 = 10^{-5} \sim 10^{-4}$ $1/\Omega$). However, the resistance changes are larger than those of the gap-closing type response for the tunneling-current type response ($1/R_0 = 10^{-7} \sim 10^{-6}$ $1/\Omega$), and the resistance change of Au/Pd nanoparticles is larger than that of Pd nanoparticles. Considering that Au is less reactive with H_2, sputtering of Au on Pd nanoparticles should have reduced the resistance change. However, it was not observed.

To understand the mechanism of the larger resistance change of Au/Pd than Pd, DFT atomistic simulation was performed. Considering that the resistance change is attributed to H_2 adsorption/absorption to the nanoparticles, we calculated the adsorption and absorption energy (W^{ADS} and W^{ABS}) for Pd, Au and Au/Pd nanoparticles through (111) surface using the following equation,

$$W^{\mathrm{ADS/ABS}} = \frac{1}{N_{\mathrm{H_2}}} \left(E_{\mathrm{surface}}^{\mathrm{ON/BEN}} - E_{\mathrm{bulk}} - N_{\mathrm{H}} \frac{E_{\mathrm{H_2}}}{2} \right). \quad (1)$$

$E_{\mathrm{surface}}^{\mathrm{ON/BEN}}$ is the potential energy of the atomic model with (111) surface and H atoms on/beneath the surface for the calculation of adsorption/absorption energy. E_{bulk} is the potential energy of the bulk model and $E_{\mathrm{H_2}}$ is the potential energy of a single H_2 molecule. N_{H} is the number of H atoms in the above atomic model with (111) surface and H atoms. All

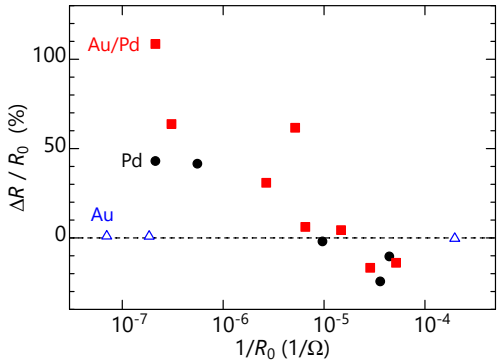

FIG. 2. Resistance change after H_2-gas flow for 231 s. H_2-gas concentration is 100 ppm.

these potential energies were calculated using the DFT simulation. Figure 3 shows the FCC atomic models with (111) surface used for calculating $E_{\mathrm{surface}}^{\mathrm{ON/BEN}}$ (24 atoms, 12 (111) layers). Referring to the stable positions of the H atoms of previous studies[17,22], two H atoms were placed at the position X on a (111) surface shown in Fig. 3 for calculating $E_{\mathrm{surface}}^{\mathrm{ON}}$, describing the fully covered surface by the hydrogen atoms, and one hydrogen atom was placed at the tetragonal site beneath the surface (position Y in Fig. 3) for calculating $E_{\mathrm{surface}}^{\mathrm{BEN}}$. To mimic the mixed surface of Au/Pd, we replaced a Pd atom in the (111) surface with an Au atom in the atomic model shown in Fig. 3 for Au/Pd case. To calculate E_{bulk}, an FCC bulk model was prepared by removing the (111) surface from the atomic model shown in Fig. 3. To calculate $E_{\mathrm{H_2}}$, a H_2 molecule was placed in a large supercell $5 \times 5 \times 5$ nm, mimicking the vacuum around it. Thus, the reference of the hydrogen state for $W^{\mathrm{ADS/ABS}}$ calculation is H_2 molecules. Although there is a previous study that considered the reference as the ionic state[23], we think our choice is reasonable for the present situation; the hydrogens will be gas molecule state in the air in our experiment. After structural relaxation (the atomic positions and cell shape) of each atomic model, we calculated the potential energies and $W^{\mathrm{ADS/ABS}}$ were derived for Pd, Au and Au/Pd cases. DFT atomistic simulations were performed using the Vienna Ab initio Simulation Package[24]. The electron–ion interaction was described using the projector-augmented wave method[25]. The exchange-correlation between electrons was treated using the Perdew–Burke–Ernzerhof generalized gradient approximation[26], with an energy cutoff of 520 eV for the plane-wave basis set. The energy convergence criteria for the electronic and ionic structure relaxations were set as 1.0×10^{-6} and 1.0×10^{-3} eV,

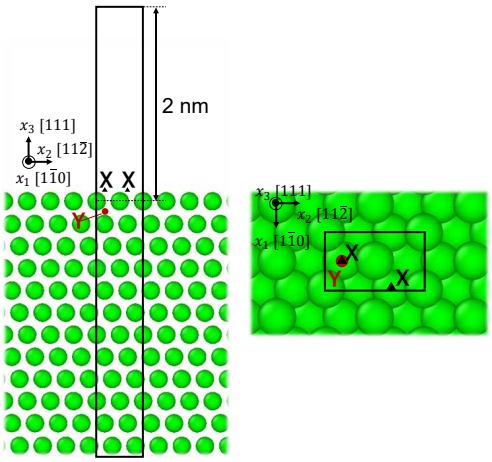

FIG. 3. Atomic models used for DFT atomistic simulation to calculate $E_{\text{surface}}^{\text{ON/BEN}}$. The black lines indicate the supercell. H atoms were put at X (black triangles) and Y (red circles) position for $E_{\text{surface}}^{\text{ON}}$ and $E_{\text{surface}}^{\text{BEN}}$ calculations, respectively. The atomic structures were visualized using the OVITO software[27].

respectively. A $10 \times 10 \times 1$ k-point mesh was used for the atomic model shown in Fig. 3 and the bulk model. A $1 \times 1 \times 1$ k-point mesh was used for the E_{H_2} calculation.

Table I shows the adsorption and absorption energies of a single H atom on (111) surfaces of Pd, Au/Pd, and Au. The adsorption energy on Pd and Au/Pd shows a negative value, indicating that dissociated H atoms can be adsorbed on their surfaces. In contrast, the adsorption energy on Au shows a positive value, indicating that H atoms cannot be adsorbed on the Au surface. Because the tunneling current is affected by the surface condition of the nanoparticles, no response to the H_2-gas flow of the nanogap Au nanoparticles can be explained by the positive adsorption energy on the Au surface. The results show that the adsorption energy of Pd is lower than that of Au/Pd. This means that the resistivity change of Pd nanoparticles would be larger than that of Au/Pd nanoparticles. However, the experimental results show the opposite behavior. Note that we also calculated the adsorption energy using the same atomic model but with only *one* hydrogen atom on the surface to investigate the effect of coverage. As a result, -0.49, -0.27 and 0.21 eV/atom for Pd, Au/Pd and Au cases were calculated. Although the value of adsorption energy decreases for all

TABLE I. The calculated values of the adsorption and absorption energy $W^{\mathrm{ADS/ABS}}$ (eV/atom).

	W^{ADS}	W^{ABS}
Pd	-0.46	-0.150
Au/Pd	-0.075	0.010
Au	0.29	(>0)

cases from those on Table I, the signs of adsorption energies do not change. Thus, we think the discussion will not change with respect to the coverage.

Next, we focus on the absorption energy. During the structural relaxation in the DFT simulation, an H atom diffused onto the Au surface, and the absorption energy could not be calculated for Au, indicating that H atoms are not absorbed by Au. Regarding Pd, the absorption energy shows the negative value, and H atoms are absorbed by Pd. Meanwhile, absorption energy of Au/Pd showed a positive value, indicating that H atoms tend to remain on the surface of Au/Pd nanoparticles. Activation energy of the hydrogen atom intrusion through the surface was also calculated for Pd and Au/Pd nanoparticles, and it was estimated to be 0.43 and 0.53 eV, respectively. Larger activation energy for Au/Pd also supports the view that H atoms tend to remain on the surface for Au/Pd nanoparticles. (Detail of the activation energy calculation is described in the supplementary material.)

From these calculations, the resistance change of Au/Pd nanoparticles is supposed to originate from the suppression of the tunneling current by the hydrogen adsorption. On the other hand, the resistance change of Pd nanoparticles is supposed to be affected by the gap narrowing by the hydrogen absorption in addition to the suppression of the tunneling current by the hydrogen adsorption. As the result, the resistance increment in Au/Pd nanoparticles tends to be larger than that in Pd nanoparticles. Considering that the adsorption energy of Pd is lower than that of Au/Pd, the adsorption rate of H atoms will be faster on Pd nanoparticles. As shown in Fig. 1, the response time, the time to reach 90% of the maximum resistance change, of Pd nanoparticles is smaller than that of Au/Pt, confirming the validity of the above interpretation.

In summary, we investigated the resistance change of nanogap Pd, Au, and Au/Pd nanoparticles under the H_2-gas flow. Since the resistance of Au remains unchanged by the H_2-gas flow, the response of Au/Pd nanoparticle was expected to be smaller than that of

Pd nanoparticles because the addition of Au on the Pd nanoparticle suppresses the adsorption of H_2 on nanoparticle surface. However, the resistance change of Au/Pd nanoparticle was larger than that of Pd nanoparticle. The DFT atomistic simulation shows that this is because on Au/Pd nanoparticle H atoms tend to remain on the nanoparticle surface, which suppresses the gap narrowing by hydrogen absorption, although H atoms tend to diffuse into pure Pd nanoparticles, causing the gap narrowing. This study demonstrates that adding less reactive material onto the nanoparticle surface does not necessarily suppress the sensing performance but may to improve it.

SUPPLEMENTARY MATERIAL

See the supplementary material for the calculation of the activation energy of the hydrogen atom intrusion through the surface of Pd and Au/Pd nanoparticles.

AUTHOR DECLARATIONS

Conflict of Interest

The authors have no conflicts to disclose.

Author Contributions

Nobutomo Nakamura Conceptualization (lead); Formal Analysis (equal); Investigation (equal); Supervision (lead); Writing/Original Draft Preparation (lead); Writing/Review & Editing (equal) **Kazushi Yoshikawa** Investigation (equal); Formal Analysis (equal); Writing/Review & Editing (equal) **Akio Ishii** Investigation (equal); Formal Analysis (equal); Software (lead); Writing/Original Draft Preparation (supporting); Writing/Review & Editing (equal)

DATA AVAILABILITY

The data that support the findings of this study are available from the corresponding author upon reasonable request.

REFERENCES

[1]B. D. Adams and A. Chen, Mater. Today **14**, 282 (2011).

[2]I. Darmadi, F. A. A. Nugroho, and C. Langhammer, ACS Sensors **5**, 3306 (2020).

[3]H.-S. Lee, J. Kim, H. Moon, and W. Lee, Adv. Mater. **33**, 2005929 (2021).

[4]F. Favier, E. C. Walter, M. P. Zach, T. Benter, and R. M. Penner, Science **293**, 2227 (2001).

[5]O. Dankert and A. Pundt, Appl. Phys. Lett. **81**, 1618 (2002).

[6]G. Kaltenpoth, P. Schnabel, E. Menke, E. C. Walter, M. Grunze, and R. M. Penner, Anal. Chem. **75**, 4756 (2003).

[7]T. Xu, M. P. Zach, Z. L. Xiao, D. Rosenmann, U. Welp, W. K. Kwok, and G. W. Crabtree, Appl. Phys. Lett. **86**, 203104 (2005).

[8]M. K. Kumar, M. S. R. Rao, and S. Ramaprabhu, J. Phys. D **39**, 2791 (2006).

[9]T. Kiefer, L. G. Villanueva, F. Fargier, F. Favier, and J. Brugger, Appl. Phys. Lett. **97**, 121911 (2010).

[10]N. Nakamura, T. Ueno, and H. Ogi, Appl. Phys. Lett. **114**, 201901 (2019).

[11]Y. K. Gautam, A. Sanger, A. Kumar, and R. Chandra, Ing. J. Hydrogen Energy **40**, 15549 (2015).

[12]K. Yu, X. Tian, X. Wang, F. Yang, T. Qi, and J. Zuo, Sens. Actuators B Chem. **299**, 126989 (2019).

[13]J. Gong, Z. Wang, Y. Tang, J. Sun, X. Wei, Q. Zhang, G. Tian, and H. Wang, J. Alloys Compd. **930**, 167398 (2023).

[14]M. Haruta, Chem. Rec. **3**, 75 (2003).

[15]T. Ishida, T. Murayama, A. Taketoshi, and M. Haruta, Chem. Rev. **120**, 646 (2020).

[16]C. Wadell, F. A. A. Nugroho, E. Lidström, B. Iandolo, J. B. Wagner, and C. Langhammer, Nano Lett. **15**, 3563 (2015).

[17]K. Namba, S. Ogura, S. Ohno, W. Di, K. Kato, M. Wilde, I. Pletikosić, P. Pervan, M. Milun, and K. Fukutani, Proc. Natl. Acad. Sci. USA **115**, 7896 (2018).

[18]N. Nakamura, N. Yoshimura, H. Ogi, and M. Hirao, J. Appl. Phys. **118**, 085302 (2015).

[19]N. Nakamura and H. Ogi, Appl. Phys. Lett. **111**, 101902 (2017).

[20]A. Ishii and N. Nakamura, J. Appl. Phys. **135**, 094301 (2024).

[21]N. Nakamura, T. Ueno, and H. Ogi, J. Appl. Phys. **126**, 225104 (2019).

[22]J. E. Mueller, P. Krtil, L. A. Kibler, and T. Jacob, Phys. Chem. Chem. Phys. **16**, 15029 (2014).

[23]A. M. Pessoa, J. L. Fajín, J. R. Gomes, and M. N. D. Cordeiro, Surf. Sci. **606**, 69 (2012).

[24]G. Kresse and J. Furthmüller, Physi. Rev. B **54**, 11169 (1996).

[25]G. Kresse and D. Joubert, Phys. Rev. B **59**, 11 (1999).

[26]J. Perdew, K. Burke, and M. Ernzerhof, Phys. Rev. Lett. **77**, 3865 (1996).

[27]A. Stukowski, Modell. Sim.Mater. Sci. Eng. **18**, 015012 (2010).